J. Fluid Mech. (1999), *vol.* 390, *pp.* 25–43. Printed in the United Kingdom

Analytical and experimental investigations of the reflection of asymmetric shock waves in steady flows

By H. LI[1,2], A. CHPOUN[3] AND G. BEN-DOR[1]

[1]Pearlstone Center for Aeronautical Engineering Studies, Department of Mechanical Engineering, Ben-Gurion University of the Negev, Beer-Sheva, Israel
[2]Department of Mechanical and Aerospace Engineering, University of California at Irvine, Irvine, CA, USA
[3]Laboratoire d'Aérothermique du CNRS, Meudon, France

(Received 9 October 1997 and in revised form 27 January 1999)

The reflection of asymmetric shock waves in steady flows is studied both theoretically and experimentally. While the analytical model was two-dimensional, three-dimensional edge effects influenced the experiments. In addition to regular and Mach reflection wave configurations, an inverse-Mach reflection wave configuration, which has been observed so far only in unsteady flows (e.g. shock wave reflection over concave surfaces or over double wedges) has been recorded. A hysteresis phenomenon similar to the one that exists in the reflection of symmetric shock waves has been found to also exist in the reflection of asymmetric shock waves. The domains and transition boundaries of the various types of overall reflection wave configurations are analytically predicted.

1. Introduction

Generally, depending on whether the flow field is steady or unsteady, the shock wave reflection phenomenon can be divided into two categories: stationary (steady) and non-stationary reflections. In the present study only steady reflections are considered.

In steady shock wave reflections, most research works (e.g. von Neumann 1945; Henderson & Lozzi 1975, 1979; Hornung, Oertel & Sandeman 1979; Hornung & Robinson 1982; Chpoun *et al.* 1995; Vuillon, Zeitoun & Ben-Dor 1995; Ivanov, Gimelshein & Beilich 1995; Li & Ben-Dor 1997; Skews 1997) have dealt with the reflection of symmetric shock waves. The state-of-the-art of these studies is as follows: Two types of wave configurations, namely regular reflection (RR) and Mach reflection (MR) have been found to exist. There are two extreme criteria, namely the *detachment criterion* and the *von Neumann criterion*, for the transition between these two types of reflections. These two criteria bound a domain inside which both the RR and the MR wave configurations are theoretically possible. For this reason the domain is referred to as the *dual solution domain*. Both the RR and the MR wave configurations are theoretically stable in the dual-solution domain (Li & Ben-Dor 1996). A two-dimensional hysteresis process in the transition can exist in the dual solution domain (Hornung *et al.* 1979). The above-mentioned two-dimensional hysteresis process has been confirmed, so far, only numerically (Ivanov *et al.* 1995). Three-dimensional edge effects contaminated all the experimental studies in which a hysteresis process in the RR → MR → RR transition was recorded (Skews 1998; Ivanov *et al.* 1998*a,b*). Consequently, the hypothesized two-dimensional hysteresis has not yet been confirmed experimentally.

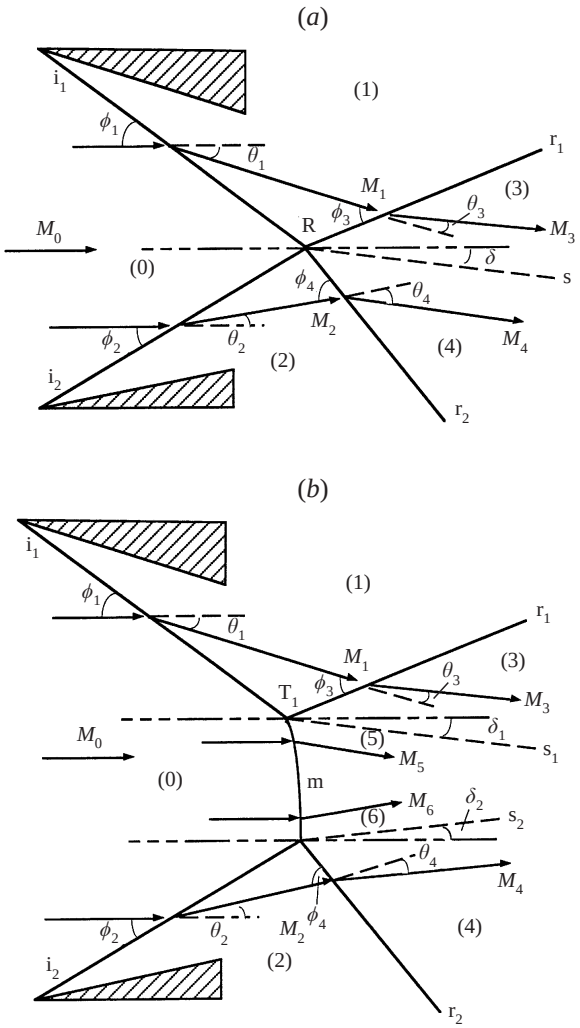

FIGURE 1. Schematic illustration of two general overall wave configurations which can be obtained from the reflection of asymmetric shock waves in steady flows and definition of the relevant parameters. (*a*) An overall regular reflection (RR), and (*b*) an overall Mach reflection (MR).

In most realistic supersonic flow situations, e.g. intake flows, nozzle flows, external flows, etc., interactions of asymmetric rather than symmetric shock waves are more likely to occur. For this reason Chpoun & Lengrand (1997) initiated an experimental study on the reflection of asymmetric shock waves. Their study revealed that, similarly to the reflection of symmetric shock waves, a hysteresis in the RR → MR → RR transition exists also in the reflection of asymmetric shock waves.

The main purpose of the present study was to provide a detailed analysis of the two-dimensional reflection of asymmetric shock waves in steady flows. Owing to the fact that some new features, which were missed by Chpoun & Lengrand's (1997) experimental study, were discovered in the course of the present analytical study, it was decided to conduct a complementary experimental investigation, in order to verify these new features.

Similarly to the interaction of symmetric shock waves in steady flows, the interaction

of asymmetric shock waves leads to two types of overall wave configurations, namely, an overall regular reflection (RR) and an overall Mach reflection (MR). These two overall wave configurations are shown, schematically, in figures 1(*a*) and 1(*b*), respectively. An overall RR wave configuration consists of two incident shock waves (i_1 and i_2), two reflected shock waves (r_1 and r_2), and one slipstream (s). These five discontinuities meet at a single point (R). The slipstream (s) results from the flow streamlines passing through unequal shock wave structures, i.e. i_1, r_1 and i_2, r_2. The flow deflection angles are θ_1, θ_2, θ_3 and θ_4 through i_1, i_2, r_1 and r_2, respectively. The boundary condition for an overall RR is

$$\theta_1 - \theta_3 = \theta_2 - \theta_4 = \delta. \tag{1}$$

When the reflection is symmetric $\theta_1 = \theta_2$ and $\delta = 0$.

In the overall MR wave configuration (figure 1*b*), in addition to the incident and reflected shock waves (i_1, i_2, r_1, r_2) a Mach stem (m) appears. It bridges two triple points (T_1 and T_2) and is complemented by two slipstreams (s_1 and s_2). The boundary conditions for an overall MR are

$$\theta_1 - \theta_3 = \delta_1 \tag{2}$$

and

$$\theta_2 - \theta_4 = \delta_2. \tag{3}$$

When the reflection is symmetric $\theta_1 = \theta_2$ and $\delta_1 = \delta_2$.

Most of the interest in the recent studies of shock wave reflections has concentrated on the transition between the RR and the MR wave configurations. The classic two- and three-shock theories of von Neumann (1963) which have been found to accurately predict the RR $\leftrightarrow$ MR transition criterion in the reflection of symmetric shock waves, will be employed also in the present study, in order to investigate the RR $\leftrightarrow$ MR transition in the reflection of asymmetric shock waves. Since the boundary conditions for the overall RR and the overall MR wave configurations in the reflection of asymmetric shock waves are different from those in the reflection of symmetric shock waves, new features can be expected to occur in the reflection of asymmetric shock waves.

2. Present study

2.1. *Shock polar analysis*

The use of pressure-deflection shock polars is very convenient for analysing phenomena involving shock wave reflections (see Ben-Dor 1991, Chapter 1.4). As shown there, the Mach reflection wave configuration can be sub-divided into three categories depending on the location of the intersection of the R-polar with the I-polar: the three possibilities are shown in figure 2. An intersection along the right-hand branch of the I-polar (e.g. point *a* in figure 2) results in a direct-Mach reflection (D_iMR). An intersection along the left-hand branch of the I-polar (e.g. point *c* in figure 2) results in an inverse-Mach reflection (I_nMR). An intersection at the point where these two branches meet, i.e. the intersection point of the I-polar with the *p*-axis (e.g. point *b* in figure 2), results in a stationary-Mach reflection (S_tMR). While in a D_iMR the slipstream and the reflection plane (e.g. the plane of symmetry in the case of the reflection of symmetric shock waves) form a converging stream tube, in an I_nMR they form a diverging stream tube. In the intermediate case of an S_tMR the slipstream is parallel to the reflecting plane.

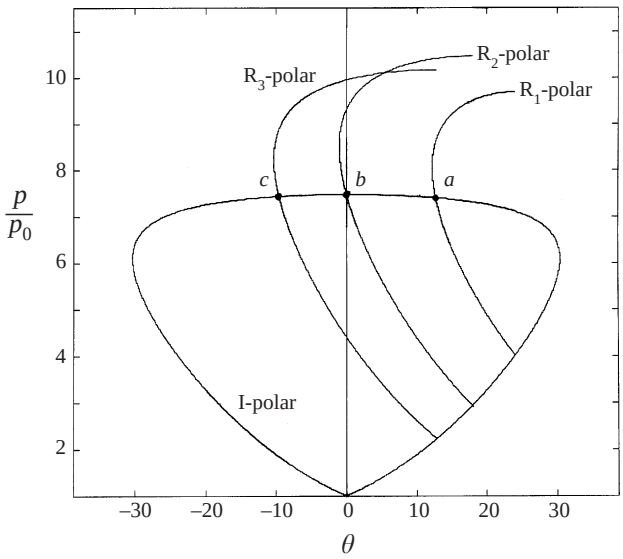

FIGURE 2. General pressure-deflection polar combinations illustrating theoretical solutions of three different types of Mach reflections: a direct-Mach reflection (D_iMR) at point *a*, a stationary-Mach reflection (S_tMR) at point *b*, and an inverse-Mach reflection (I_nMR) at point *c*.

The pressure and the deflection angle across an oblique shock wave are related as follows (see Han & Yin 1993, p. 235):

$$\theta = \pm f(\gamma, M, \xi) \tag{4}$$

where

$$f(\gamma, M, \xi) = \arctan\left\{\frac{(\xi-1)^2[2\gamma(M^2-1)-(\gamma+1)(\xi-1)]}{[\gamma M^2-(\xi-1)]^2[2\gamma+(\gamma+1)(\xi-1)]}\right\}^{1/2}. \tag{5}$$

Here γ, M, ξ and θ are the specific heat capacities ratio, the flow Mach number ahead of the shock wave, the pressure ratio across the shock wave and the flow deflection angle, respectively. The positive and negative signs in equation (4) correspond to counter-clockwise and the clockwise deflection angles, respectively.

The tangent of the shock polar in the (ξ, θ)-plane can be obtained by differentiating equation (4) with respect to ξ, i.e.

$$\frac{\mathrm{d}\theta}{\mathrm{d}\xi} = \pm g(\gamma, M, \xi) \tag{6}$$

where

$$g(\gamma, M, \xi) = \frac{4\gamma(M^2-1)-(\gamma+1)(4-M^2)(\xi-1)-(\gamma+1)(\xi-1)^2}{[2\gamma(M^2-1)-(\gamma+1)(\xi-1)]^{1/2}[2\gamma+(\gamma+1)(\xi-1)]^{1/2}} \times \left\{2\gamma M^2-[4-(\gamma+1)M^2](\xi-1)-2(\xi-1)^2\right\}^{-1}. \tag{7}$$

Equations (6) and (7) will be used, in the subsequent discussion, to define the domains of the various wave configurations associated with the reflection of asymmetric shock waves.

In the following the theoretically possible wave configurations which can result from the reflection of asymmetric shock waves will be analysed with the aid of shock polars.

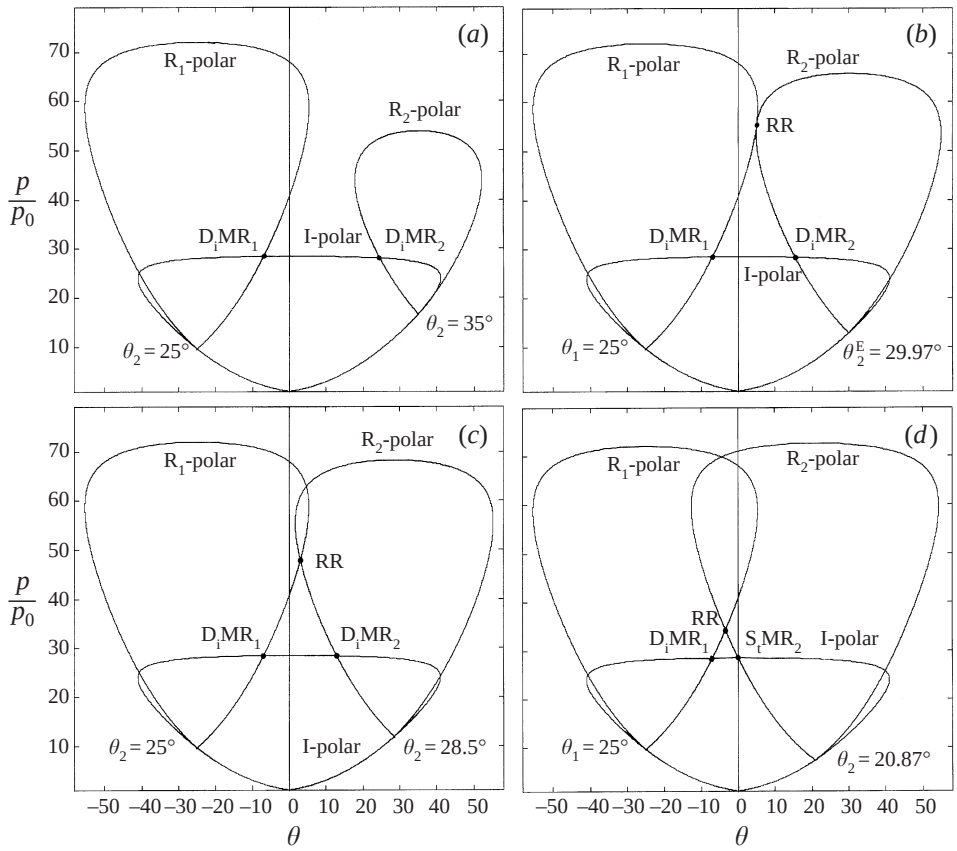

FIGURE 3. for caption see facing page.

Figures 3(*a*)–3(*g*) illustrate seven shock polar combinations. For all the combinations the flow Mach number is $M_0 = 4.96$ and hence the I-polar is identical. Furthermore, since the angle of one reflecting wedge is kept constant at $\theta_1 = 25°$, all the R_1-polars are also identical. Note that the intersection of the I- and the fixed R_1-polars predicts a direct-Mach reflection (D_iMR) as shown in figures 3(*a*)–3(*g*).

The shock polar combination of figure 3(*a*) is for $M_0 = 4.96$, $\theta_1 = 25°$ and $\theta_2 = 35°$. As can be seen the intersection of the R_2- and the I-polars results in a D_iMR. Consequently, the shock polar combination shown in figure 3(*a*) represents the solution of an overall Mach reflection wave configuration that consists of two direct-Mach reflections. A schematic illustration of this overall MR wave configuration is shown in figure 4(*a*). Note that since the overall Mach reflection wave configuration consists of two direct-Mach reflections their slipstreams form a converging stream tube. Hence the subsonic flow behind the Mach stem accelerates, similarly to the situation obtained in the reflection of symmetric shock waves.

When θ_2 is decreased to 29.97° the shock polar combination shown in figure 3(*b*) is obtained. Here the R_1- and R_2-polars are tangent to each other. As a result, in addition to an overall Mach reflection wave configuration, similar to that shown in figure 4(*a*) which consists of two direct-Mach reflections (D_iMR_1 and D_iMR_2), here an overall regular reflection wave configuration at the point where the R_1- and R_2-polars are tangent to each other is also theoretically possible. The shock polar combination

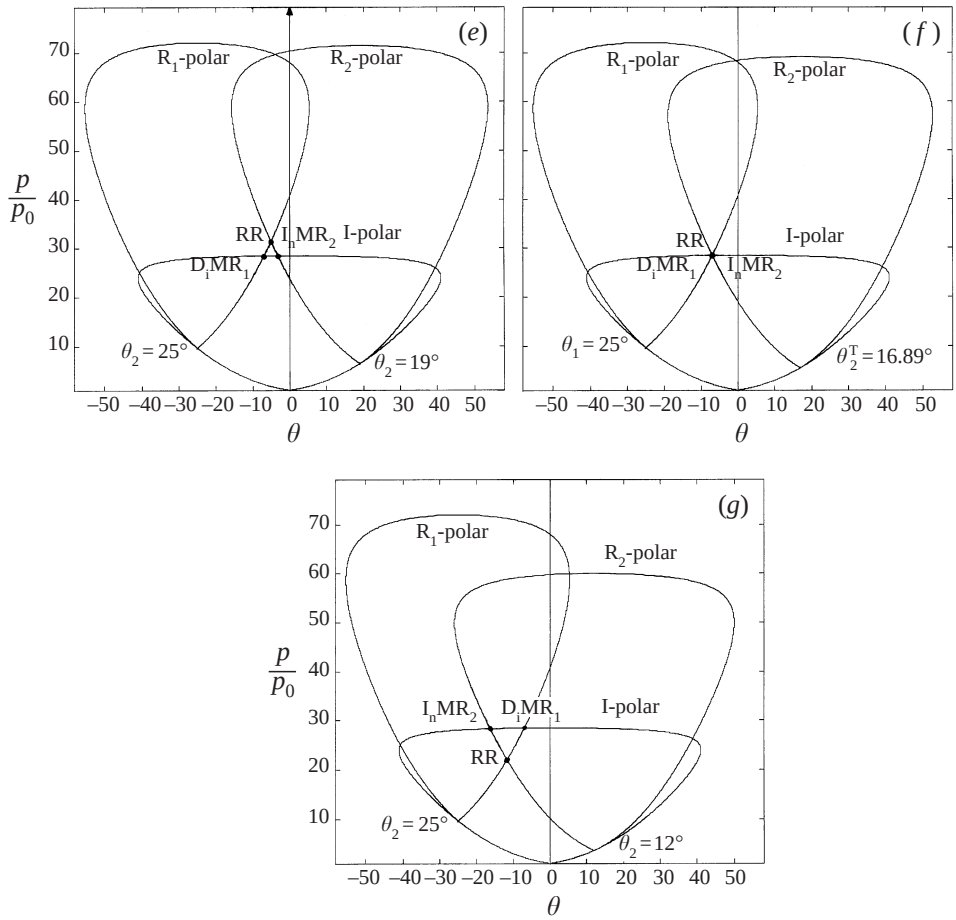

FIGURE 3. Pressure-deflection polar combinations illustrating various theoretically possible solutions in the reflection of asymmetric shock waves for a fixed flow Mach number $M_0 = 4.96$ and one fixed wedge angle $\theta_1 = 25°$. (*a*) An overall MR that consists of two direct-Mach reflections (D_iMR) for $\theta_2 = 35°$. (*b*) An overall RR or an overall MR that consists of two D_iMR for $\theta_2 = 29.97°$. Note that this situation is analogous to the detachment condition. (*c*) An overall RR or an overall MR that consists of two D_iMR for $\theta_2 = 28.5°$. (*d*) An overall RR or an overall MR that consists of one D_iMR and one stationary-Mach reflection (S_tMR) for $\theta_2 = 20.87°$. (*e*) An overall RR or an overall MR that consists of one D_iMR and one inverse-Mach reflection (I_nMR) for $\theta_2 = 19°$. (*f*) An overall RR or an overall MR that consists of one D_iMR and one I_nMR for $\theta_2 = 16.89°$. Note that this situation is analogous to the von Neumann condition. (*g*) An overall RR or an overall MR that consists of one D_iMR and one I_nMR for $\theta_2 = 12°$. Note that (*b*), (*c*), (*d*), (*e*) and (*f*) correspond to the dual-solution domain.

shown in figure 3(*b*) is analogous to the *detachment* condition in the reflection over a single wedge or the reflection of symmetric shock waves (see Ben-Dor 1991).

When θ_2 is further decreased to 28.5° the shock polar combination shown in figure 3(*c*) is reached. Here again both an overall MR wave configuration which consists of two direct-Mach reflections (D_iMR_1 and D_iMR_2) and an overall RR wave configuration are theoretically possible.

Upon a further decrease in θ_2, to 20.87°, the situation shown in figure 3(*d*) is obtained. Similarly to the cases shown in figures 3(*b*) and 3(*c*), the overall reflection here again can be either an overall MR or an overall RR. However, unlike

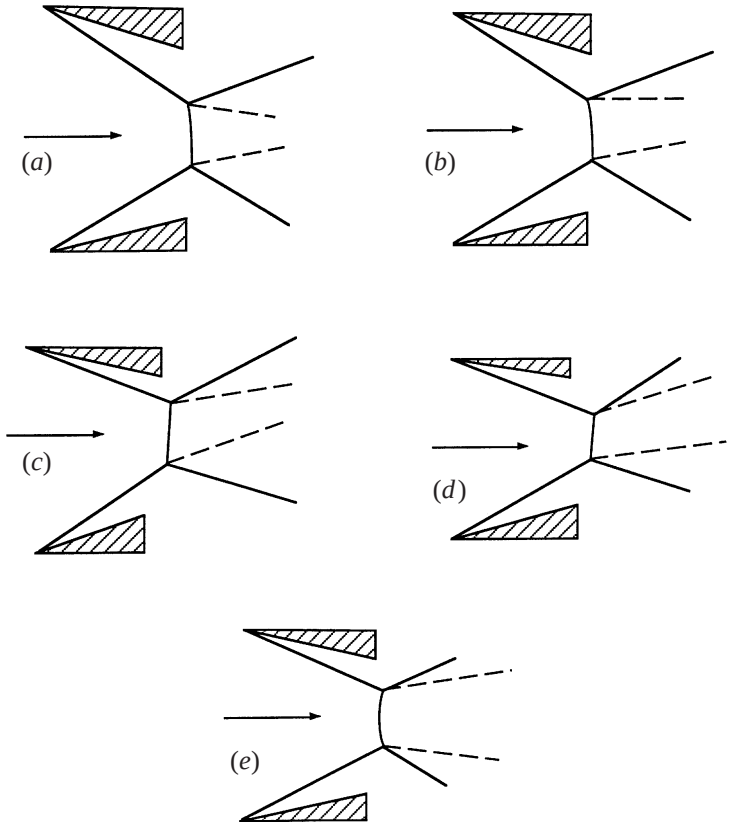

FIGURE 4. Schematic illustration of the wave configurations of various overall Mach reflections consisting of: (*a*) two D_iMR, (*b*) one D_iMR and one S_tMR, (*c*) one D_iMR and one I_nMR with a converging slipstream tube, (*d*) one D_iMR and one I_nMR with a diverging slipstream tube, (*e*) two I_nMR. Note that the wave configurations shown in (*d*) and (*e*) are not physical.

those cases, where the overall MR wave configuration consisted of two direct-Mach reflections (D_iMR_1 and D_iMR_2), here the overall MR wave configuration consists of a direct-Mach reflection (D_iMR_1) and a stationary-Mach reflection (S_tMR_2). A schematic illustration of the overall wave configuration corresponding to this case is shown in figure 4(*b*). Note that the slipstream of the stationary-Mach reflection wave configuration is parallel to the oncoming flow. Similarly to the wave configuration shown in figure 4(*a*) the two slipstreams in figure 4(*b*) also form a converging stream tube.

A further decrease in θ_2, to 19°, results in the situation shown in figure 3(*e*). Again two solutions are theoretically possible: an overall RR or an overall MR. However, unlike the previously described cases, here the overall MR wave configuration consists of a direct-Mach reflection (D_iMR_1) and an inverse-Mach reflection (I_nMR_2). A schematic drawing of the overall wave configuration corresponding to this case is shown in figure 4(*c*). Note the orientation of the slipstream of the InMR, which is shown in the upper part of figure 4(*c*). It should be noted here again that the stream tube formed by the two slipstreams is converging.

An interesting shock polar combination is obtained when θ_2 is further decreased and reaches the value 16.89°. At this condition the three polars, namely the I-, R_1- and R_2-polars meet at a single point as shown in figure 3(*f*). This combination is, in

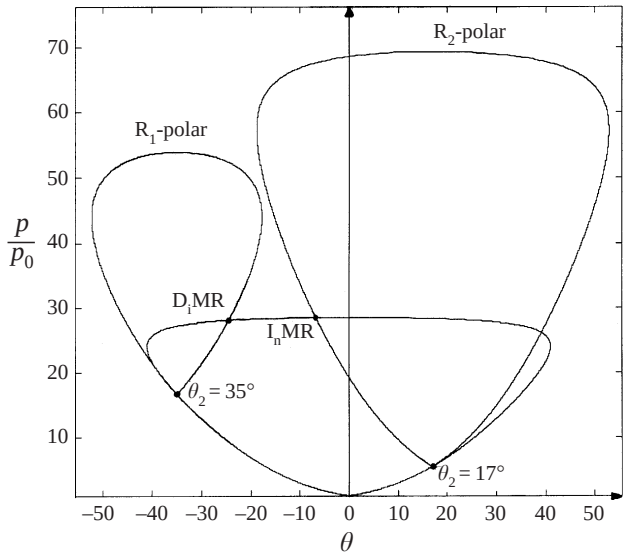

FIGURE 5. Pressure-deflection polar combinations illustrating an overall MR consisting of one D_iMR and one I_nMR for $M_0 = 4.96$, $\theta_1 = 35°$ and $\theta_2 = 17°$.

fact, analogous to the *von Neumann* condition in the reflection over a single wedge or the reflection of symmetric shock waves (see Ben-Dor 1991).

Based on the foregoing discussion, the shock polar combinations shown in figures 3(*b*) and 3(*f*) are the two extreme situations between which both an overall RR and an overall MR wave configurations are theoretically possible. Hence, they are, in fact, the upper ($\theta_2 = 29.97°$, see figure 3*b*) and the lower ($\theta_2 = 16.89°$, see figure 3*f*) bounds of the dual-solution domain for $M_0 = 4.96$ and $\theta_1 = 25°$.

When θ_2 is further reduced, e.g. to 12°, the resulting shock polar combination, which is shown in figure 3(*g*), suggests an overall RR wave configuration at the point where the R_1- and R_2- polars intersect. The other theoretical solution suggested by this shock polar combination, i.e. an overall MR wave configuration, which consists of a D_iMR_1 and an I_nMR_2, is not physical since it implies a wave configuration in which the slipstreams of the two MR wave configurations form a diverging stream tube (see figure 4*d*). Such a stream tube cannot be negotiated by the subsonic flow behind the Mach stem.

2.2. *Special types of shock wave reflections*

Based on the foregoing shock polar analysis, overall MR wave configurations consisting of one D_iMR and one I_nMR are theoretically possible for shock polar combinations such as the one shown in figure 3(*e*) which, as mentioned earlier, corresponds to the dual-solution domain (i.e. an overall RR wave configuration is also possible for this shock polar combination). Unlike the combination shown in figure 3(*e*), the shock polar combination for $M_0 = 4.96$, $\theta_1 = 35°$ and $\theta_2 = 17°$ which is shown in figure 5, represents a solution in which only an overall MR wave configuration, consisting of one D_iMR and one I_nMR is theoretically possible. A schematic illustration of this overall reflection is shown in figure 4(*c*). It should be mentioned here that in the reflection of two symmetric shock waves an I_nMR is not physical because the subsonic flow behind the Mach stem cannot negotiate a diverging steam tube.

Another interesting situation is obtained for conditions slightly different from those

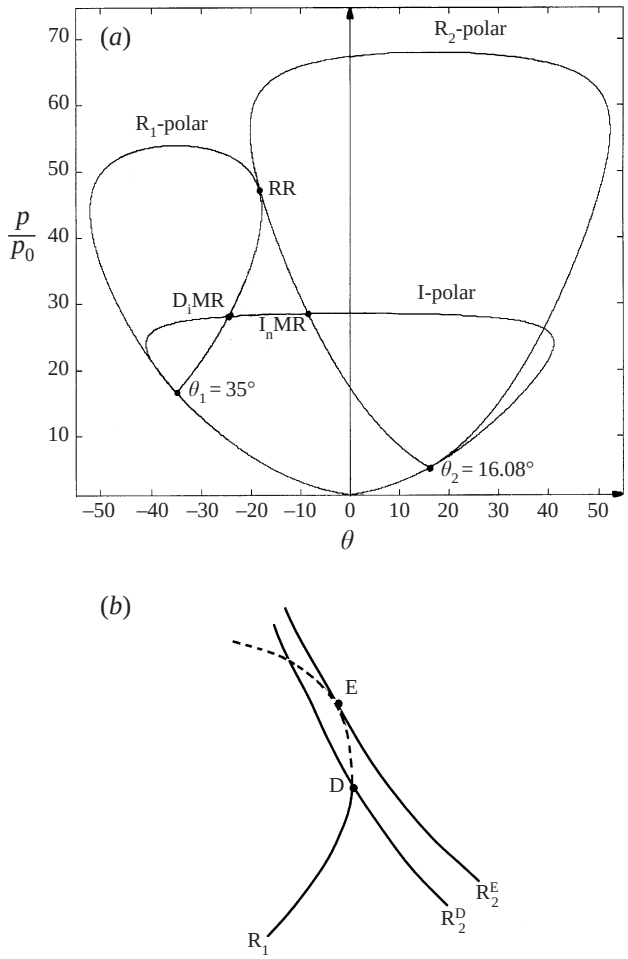

FIGURE 6. (*a*) Pressure-deflection polar combinations illustrating an overall RR that consists of one weak RR and one strong RR, and an overall MR that consists of one D_iMR and one I_nMR for $M_0 = 4.96$, $\theta_1 = 35°$ and $\theta_2 = 16.08°$. (*b*) Detailed drawing of the area of intersection in which the resulting overall RR consists of one weak RR and one strong RR.

shown in figure 5, i.e. $M_0 = 4.96$, $\theta_1 = 35°$ and $\theta_2 = 16.08°$, as shown in the shock polar combination in figure 6(*a*). Now the R_1- and R_2-polars are tangent and hence an overall RR wave configuration is theoretically possible at their point of tangency. A close inspection of figure 6(*a*) indicates that the point of tangency is on the strong shock portion of the R_1-polar and on the weak-shock portion of the R_2-polar. Hence, the overall RR wave configuration there consists of one strong RR and one weak RR.

A detailed enlargement of the vicinity of the point of tangency of the R_1- and R_2-polars is shown in figure 6(*b*) where two R_1- and R_2-polar combinations, i.e. R_1 and R_2^D and R_1 and R_2^E, are shown. While the R_1- and the R_2^E-polars are tangent the R_2^D-polar intersects the R_1-polar at its point of maximum deflection (point D). Hence any R_2-polar between the R_2^D- and the R_2^E-polars would intersect the R_1-polar along its strong-shock portion (shown in figure 6*b* as a dashed line), resulting in an overall RR wave configuration with a strong RR on the R_1-polar and a weak RR

on the R_2-polar. It is important to note that the range in which such an overall RR wave configuration is possible is very narrow. For example, for $M_0 = 4.96$ and $\theta_1 = 35^\circ$, the R_1- and R_2^D-polar combination is obtained with $\theta_2 = 15.72^\circ$ and the R_1- and R_2^E-polar combination is obtained with $\theta_2 = 16.08^\circ$. Consequently, recording this special overall RR wave configuration experimentally is not an easy task.

It should be noted that owing to the violation of the principle of minimum entropy production, a strong RR cannot be obtained in the reflection of symmetric shock waves, in steady flows, unless special pressure boundary conditions are imposed on the flow field downstream of the reflection point (for details see Salas & Morgan 1983). However, when asymmetric shock waves reflect, as is the case in the present study, the complementary weak RR is capable of providing, behind its reflected shock wave, the high pressure which is required to support a strong RR. For example, consider figure 1(*a*) and assume that the upper RR is weak and the lower RR is strong. Based on the above explanation, it is possible that the weak RR will result, in region 3 behind its reflected shock wave, in a pressure which will be sufficient to provide the high pressure required in region 4 to support a strong RR. Note that the pressures across the slipstream s are equal. i.e. $p_2 = p_3$.

Finally, it should also be noted here that because an overall MR wave configuration having diverging slipstreams cannot exist, an overall MR wave configuration which consists of two inverse-Mach reflections, such as the one shown schematically in figure 4(*e*) is not physical.

2.3. *Transition criterion*

Based on the foregoing discussion the 'detachment' condition (i.e. the condition at which the R_1- and R_2-polars are tangent, see figure 3*b*) can be expressed mathematically as

$$f(\gamma, M_1, p/p_1) + f(\gamma, M_2, p/p_2) + \theta_1 - \theta_2 = 0, \tag{8}$$

$$g(\gamma, M_1, p/p_1) + g(\gamma, M_2, p/p_2) = 0. \tag{9}$$

Similarly, the mathematical expression for the von Neumann condition (i.e. the condition at which the I-, R_1- and R_2-polars meet at the same point, see figure 3*f*) is given by

$$f(\gamma, M_0, p/p_0) + f(\gamma, M_1, p/p_1) + \theta_1 = 0, \tag{10}$$

$$f(\gamma, M_0, p/p_0) - f(\gamma, M_2, p/p_2) + \theta_2 = 0, \tag{11}$$

where, based on the oblique shock wave relations, p_1, p_2, M_1, M_2 are given by

$$p_j = \frac{p_0}{\gamma + 1}[2M_0^2 \sin^2 \phi_j - (\gamma - 1)], \tag{12}$$

$$M_j = \frac{\{1 + (\gamma - 1)2M_0^2 \sin^2 \phi_j + [\frac{1}{4}(\gamma + 1)^2 - \gamma \sin^2 \phi_j]M_0^4 \sin^2 \phi_j\}^{1/2}}{\left[\gamma M_0^2 \sin^2 \phi_j - \dfrac{\gamma - 1}{2}\right]^{1/2} \left[\dfrac{\gamma - 1}{2} M_0^2 \sin^2 \phi_j + 1\right]^{1/2}}, \tag{13}$$

and the relation between ϕ_j and θ_j is given by

$$\tan \theta_j - \frac{2 \cot \phi_j (M_0^2 \sin^2 \phi_j - 1)}{M_0^2(\gamma + \cos 2\phi_j) + 2} = 0. \tag{14}$$

Here, $j = 1$ and 2 for the upper and the lower reflections, respectively.

The 'detachment' transition line given by expressions (8) and (9) and the 'von

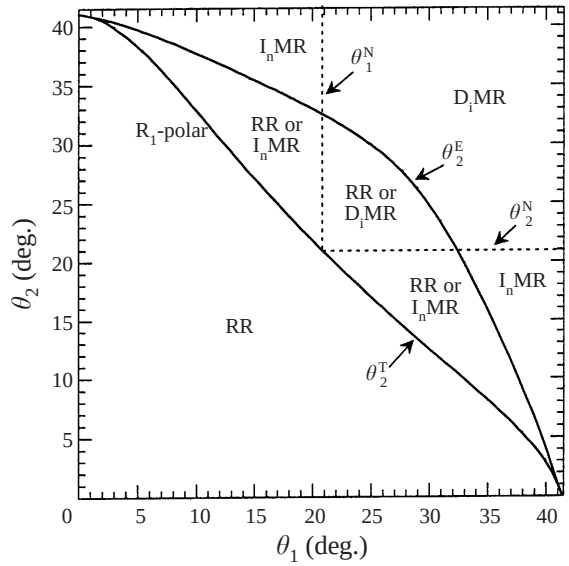

FIGURE 7. The dual-solution domain in the (θ_1, θ_2)-plane for $M_0 = 4.96$. The transition lines θ_2^E and θ_2^T correspond to the shock polar combinations shown in figures 3(*b*) and 3(*f*), respectively.

Neumann' transition line given by expressions (10) and (11) are drawn as solid lines in figure 7 in the (θ_1, θ_2)-plane for $M_0 = 4.96$. The lines are labelled θ_2^E and θ_2^T, respectively. The earlier mentioned dual solution domain, inside which the overall wave configuration can be either a regular reflection or a Mach reflection, extends between these two transition lines.

The two dashed lines marked θ_1^N and θ_2^N indicate the 'von Neumann' condition for a symmetric reflection, e.g. the shock polar combination shown in figure 3(*d*) where $\theta_2 = \theta_2^N$ is a point on the dashed line. On one side of the dashed line the Mach reflection is direct and on the other side it is inverse.

Based on figure 7 the dual-solution domain can be divided into two parts (note the symmetry between the wedge angles θ_1 and θ_2). In one part, labelled as RR or D_iMR, the overall wave configuration can be either an RR or an MR which consists of two direct-Mach reflections, as shown in figure 4(*a*). In the other part, labelled RR or I_nMR, the overall wave configuration can be either an RR or an MR which consists of one direct-Mach reflection and one inverse-Mach reflection, as shown in figure 4(*c*). Note that in both cases the slipstreams of the two Mach reflections, of which the overall MR wave configuration consists, form converging stream tubes.

The domains of different types of overall wave configurations are shown in the (M_0, θ_2)-plane for $\theta_1 = 15°$, $20°$ and $25°$ in figures 8(*a*), 8(*b*) and 8(*c*), respectively. It is evident from these figures that for a fixed wedge angle, θ_1, different sequences of overall wave configurations can be encountered as θ_2 is changed for a fixed flow Mach number, M_0. Consider, for example, the case shown in figure 8(*a*) for $\theta_1 = 15°$. The vertical line $M_0^D(\theta_1)$ indicates the lowest flow Mach number for which an attached oblique shock wave is possible over the fixed wedge (i.e. the wedge having the angle θ_1). For the case shown in figure 8(*a*) one can easily calculate $M_0^D(\theta_1) = 1.62$. The line θ_2^D indicates the largest value of the angle of the other wedge for which an attached shock wave can be obtained for any given flow Mach number, M_0. The vertical line $M_0^N(\theta_1)$ indicates the flow Mach number for which the Mach reflection over the fixed

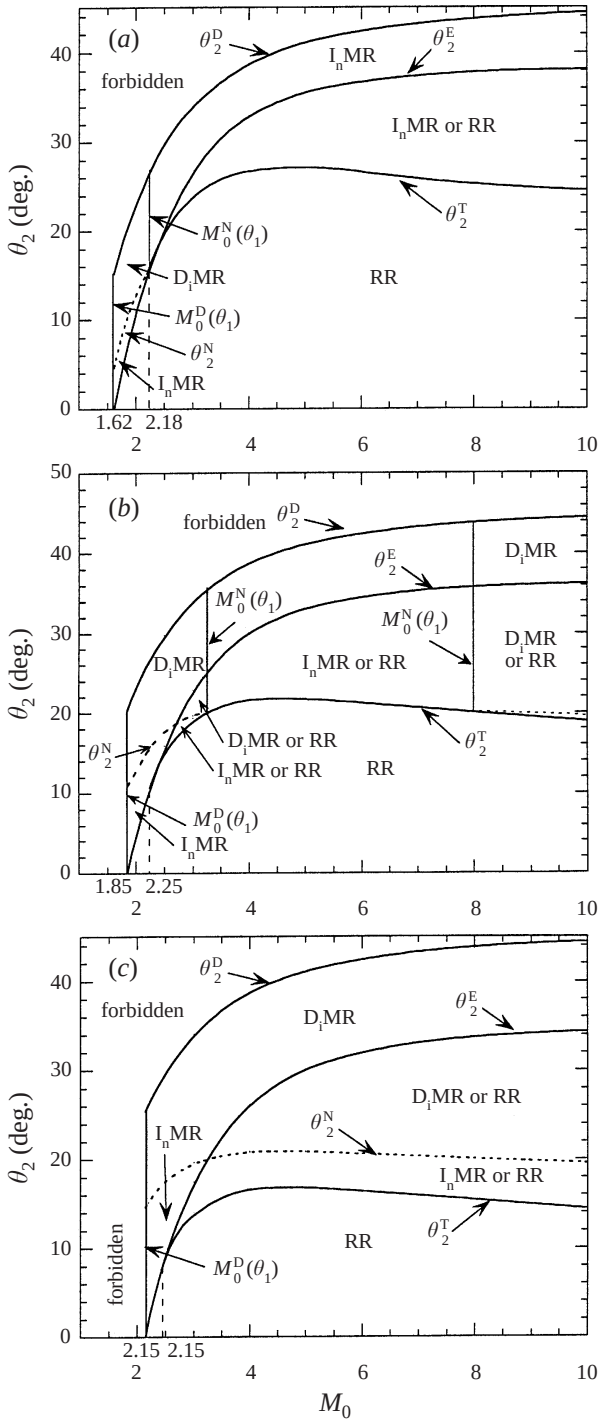

FIGURE 8. Domains of various types of reflections in the (M_0, θ_2)-plane for (*a*) $\theta_1 = 15°$, (*b*) $\theta_1 = 20°$, and (*c*) $\theta_1 = 25°$.

wedge (i.e. the wedge having the angle θ_1) is a stationary-Mach reflection (S_tMR). (For the case shown in figure 8(*a*), $M_0^N(\theta_1) = 2.18$). Similarly, the line θ_2^N indicates the value of the angle of the other wedge at which an S_tMR is obtained for any given flow Mach number, M_0.

Based on the foregoing discussion regarding the different boundary lines in the (M_0, θ_2)-plane it is clear that depending on the flow Mach number, M_0, different sequences of overall reflection wave configurations can be encountered as θ_2 is changed.

For $M_0^D(\theta_1) < M_0 < M_0^N(\theta_1)$ one obtains: a regular reflection for $0 < \theta_2 < \theta_2^E$, an inverse-Mach reflection for $\theta_2^E < \theta_2 < \theta_2^N$, and a direct-Mach reflection for $\theta_2^N < \theta_2 < \theta_2^D$.

For $M_0 > M_0^N(\theta_1)$ one gets: a regular reflection for $0 < \theta_2 < \theta_2^T$, an inverse-Mach or a regular reflection for $\theta_2^T < \theta_2 < \theta_2^E$, and an inverse-Mach reflection for $\theta_2^E < \theta_2 < \theta_2^D$.

The boundary lines described above, i.e. θ_2^D, θ_2^E, θ_2^T, θ_2^N, $M_0^D(\theta_1)$ and $M_0^N(\theta_1)$ also appear in figures 8(*b*) and 8(*c*). Owing to the change in the value of the fixed angle, θ_1, the boundary lines in figures 8(*b*) and 8(*c*) are shifted with respect to their location in figure 8(*a*). As a consequence, their intersections lead to a different variety of domains of overall reflection wave configurations. The variety of the sequences of events, as θ_2 is changed, is self-explanatory in view of the foregoing description of figure 8(*a*).

2.4. *Hysteresis phenomenon*

Similarly to the hysteresis phenomenon first hypothesized by Hornung *et al.* (1979) in the steady reflection of symmetric shock waves, a hysteresis phenomenon can be hypothesized in the present case of steady reflection of asymmetric shock waves.

Consider figure 7 and note that one could start with an overall MR wave configuration with a value of θ_2 larger than θ_2^E and then decrease θ_2 until the von Neumann transition line (θ_2^T), below which an overall MR wave configuration is theoretically impossible, will be reached. At this line the overall MR wave configuration must change to an overall RR wave configuration. If the direction of the change in θ_2 was now reversed and θ_2 increased, the overall RR wave configuration could continue to exist until the detachment line (θ_2^E), above which an overall RR wave configuration is theoretically impossible, was reached. At this line the overall RR wave configuration must change to an overall MR wave configuration.

Based on figure 7, which is drawn for $M_0 = 4.96$, it is evident that two sequences of transition of the overall reflection wave configuration are possible during the process of first decreasing θ_2 and then increasing it back to its initial value, depending on whether θ_1 is smaller or larger than θ_1^N. While for $\theta_1 < \theta_1^N = 20.87^\circ$ the overall reflection wave configuration follows the following sequence of events:

$$I_nMR \rightarrow RR(\text{at } \theta_2^T) \rightarrow I_nMR(\text{at } \theta_2^E),$$

for $\theta_1 > \theta_1^N = 20.87^\circ$ the overall reflection wave configuration follows the following sequence of events:

$$D_iMR \rightarrow I_nMR(\text{at}\, \theta_2^N) \rightarrow RR(\text{at } \theta_2^T) \rightarrow D_iMR(\text{at } \theta_2^E)$$

2.5. *The experimental study*

As indicated in the Introduction, Chpoun & Lengrand's (1997) experimental investigation of the reflection of asymmetric shock waves triggered the present study, the main purpose of which was to provide a detailed analysis of the two-dimensional reflection of asymmetric shock waves in steady flows. Furthermore, as some new

features which were missed by Chpoun & Lengrand (1997) were revealed in the course of the present analytical study, it was decided to conduct a complementary experimental investigation, in order to verify these new features.

Chpoun & Lengrand's (1997) experimental investigation was conducted in the same facility that was used by Chpoun *et al.* (1995) for their experimental investigation of the reflection of steady symmetric shock waves. The inlet aspect ratio in Chpoun & Lengrand's (1997) experimental set-up was 0.7. Since Fomin *et al.* (1996) and Skews (1997) showed that the experimental results of Chpoun *et al.* (1995) were contaminated by three-dimensional edge effects and hence could not be considered as purely two-dimensional an attempt to eliminate such effects was made.

Based on Skews' (1997) recent theoretical study an inlet aspect ratio of at least 0.75 is adequate to avoid three-dimensional edge effects from intruding to the flow field in the area of interest, for $M_0 = 4.96$. A modified recent analytical study by Skews (1998) showed that even an aspect ratio of 1 would not be suffieient to eliminate three-dimensional edge effects. Fomin *et al.* (1996) showed experimentally that three-dimensional influences extend beyond this theoretical limit. Based on their experiments an inlet aspect ratio of at least 1.25 is needed to avoid such effects†. Consequently, in order to improve the reflecting plates, which were used as shock generators and thereby reduce possible three-dimensional effects, new plates with an inlet aspect ratio 1.4 times larger than that used by Chpoun & Lengrand (1997), were used in the course of the present experimental investigation. While the width of the plates used by Chpoun & Lengrand (1997) was 50 mm the width of the new plates was 70 mm. The distance between the two leading edges of the two reflecting plates was kept constant at about 71 mm. Therefore the inlet aspect ratio for the present experiments was about 1. This value is well beyond the above-mentioned theoretical requirement of at least 0.75 but still below the experimentally based recommendation of at least 1.25.

Consequently, the experimental results, which are reported in the following, are probably contaminated with three-dimensional edge effects and hence should not be considered as purely two-dimensional. Therefore, although they cannot be, and were not, used for verifying the findings of the two-dimensional analysis, e.g. the hypothesized two-dimensional hysteresis, since they do illustrate the results of an actual hysteresis in a two/three-dimensional steady supersonic flow they will be compared with the analytical results of a purely two-dimensional flow.

2.5.1. *The experimental set-up*

The experiments were conducted on the SH2 wind tunnel of CNRS at Meudon, France. This is an open jet facility that produces a uniform airflow at Mach number 4.96 in a continuous manner. The nozzle exit diameter is 127 mm. The stagnation temperature and pressure were 453 K and 8.5 bars, respectively, leading to a Reynolds number of $1.27 \times 107\ \mathrm{m}^{-1}$.

A colour schlieren photography system connected simultaneously to a video

† It should be noted here, that while Fomin *et al.* (1996) used a closed wind tunnel, the present experiments were conducted in an open jet facility. Hence, it is important to establish what effect this different boundary condition has on the size of the minimum inlet aspect ratio required for the reflection process to be free of three-dimensional edge effects. It is also important to note that while Fomin *et al.* (1996) and Skews' (1997) studies dealt with the reflection of symmetric shock waves, the present study deals with the reflection of asymmetric shock waves, in which special pressure conditions can be imposed on the flow field downstream of the reflection point of an overall RR or the Mach stem of an overall MR. For these reasons the question of by how much the present experimental results are influenced by three-dimensional edge effects needs further investigation.

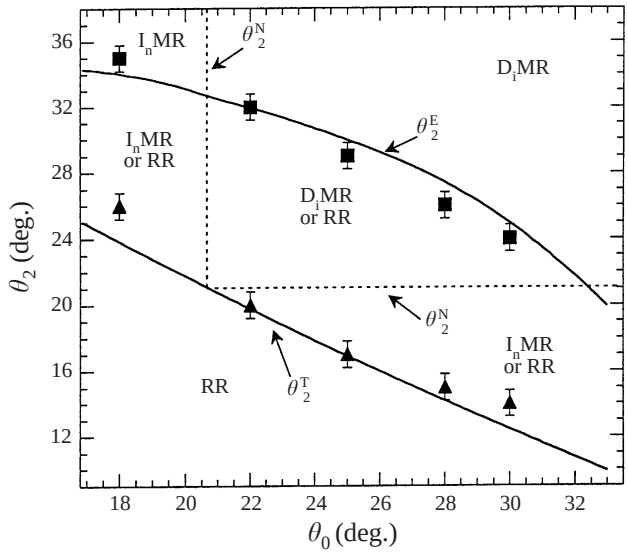

FIGURE 9. Comparison between the two-dimensional analytical transition line and the three-dimensional edge affected experiments for $M_0 = 4.96$ in the (θ_1, θ_2)-plane. Solid squares, experimentally recorded RR → MR transition points; solid triangles, experimentally recorded MR → RR transition points.

recorder and a digital picture acquisition system were employed to record the entire sequence of each experiment.

The two incident shock waves were generated using two flat plates, which were 40 mm long. They were mounted on a special rotation mechanism, connected to electric motors, by which they could be placed at any predetermined angle or could be continuously rotated around the axes aligned with their leading edges. As mentioned earlier the inlet aspect ratio was about 1. The wedge angles were measured using two digital transducers with an accuracy better than 0.3°. The inlet flow rate was kept constant during the course of each experiment.

2.5.2. *Experimental results*

The existence of a hysteresis process was checked experimentally using the following procedure. The upper wedge angle was kept constant at θ_1. The lower wedge angle θ_2 was decreased continuously from an initial value larger than θ_2^E (i.e. at which, based on a two-dimensional analysis, only an overall MR is theoretically possible) to a value smaller than θ_2^T (i.e. at which, based on a two-dimensional analysis, only an overall RR is theoretically possible). Then the direction of the change in θ_2 was reversed and the lower wedge angle was increased until it reached again its initial value.

Five different values of θ_1, namely 18°, 22°, 25°, 28° and 30°, were selected. For each of these values of θ_1 the values of θ_2 at which the actual MR → RR and RR → MR transitions took place were recorded. The results are shown in figure 9. The triangles and the squares represent the points at which the MR → RR and the RR → MR transitions were recorded, respectively. A clear hysteresis is evident in the RR ⇔ MR transition. The part of figure 7 extending from $\theta_1 = 17°$ to 33° and $\theta_2 = 11°$ to 37° has also been added to figure 9. The agreement between the analytically predicted transition lines, θ_2^E and θ_2^T, and the experimental results is surprisingly

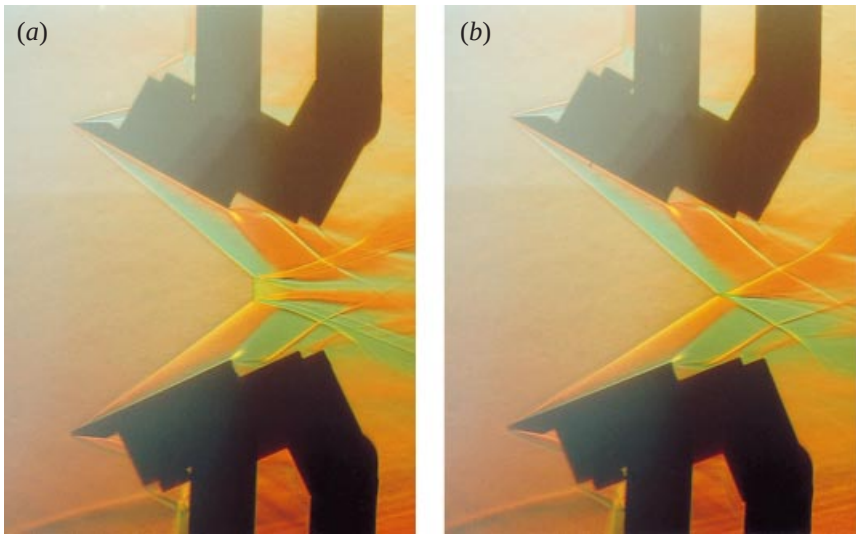

FIGURE 10. Colour schlieren photographs showing (*a*) an overall MR and (*b*) an overall RR for the same conditions. $M_0 = 4.96$, $\theta_1 = 28^\circ$ and $\theta_2 = 24^\circ$.

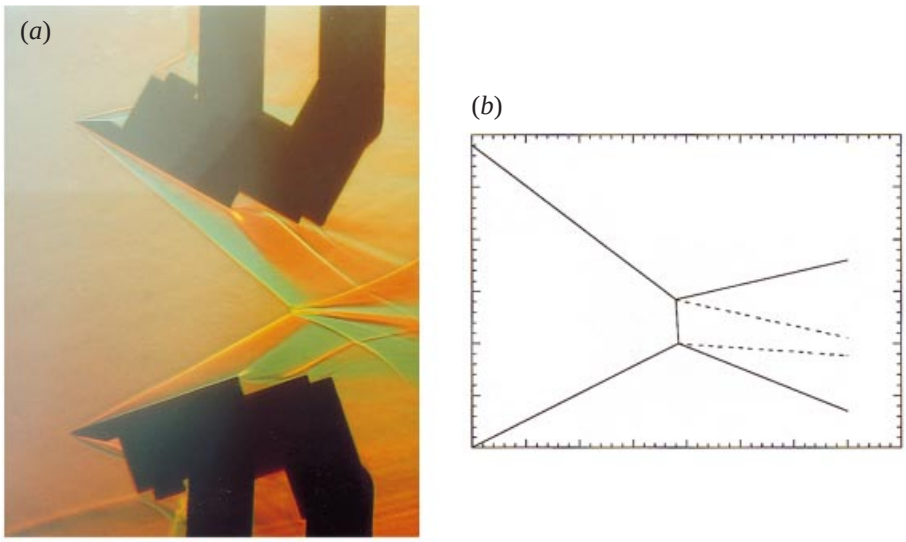

FIGURE 11. An overall MR that consists of one D_iMR and one I_nMR for $M_0 = 4.96$, $\theta_2 = 28^\circ$ and $\theta_2 = 18^\circ$. (*a*) A colour schlieren photograph and (*b*) a line drawing.

good in view of the fact that the analytical transition lines were calculated using a two-dimensional model and the experimental results are most likely contaminated with three-dimensional edge effects. The good agreement could imply either that such effects are not very dominant in our experimental set-up, and hence that the present experiments could in practice be treated as two-dimensional or that the actual MR → RR and RR → MR transition angles in three-dimensional flows are close to those of two-dimensional flows. Whether these two possibilities are general or limited to the flow Mach number at which the above-described comparison was made, i.e. $M_0 = 4.96$, is yet to be investigated.

	θ_1 (deg.)	ω_1 (deg.)	δ_1 (deg.)	θ_2 (deg.)	ω_2 (deg.)	δ_2 (deg.)
Experimental	28	11.5 ± 0.3	11 ± 0.3	18	19 ± 0.3	-5 ± 0.3
Analytical	28	12.86	12.03	18	21.99	-4.98

TABLE 1. Comparison of the experimental and the calculated results for an overall MR that consists of a D_iMR and an I_nMR for $M_0 = 4.96$, $\theta_1 = 28^\circ$ and $\theta_2 = 18^\circ$. Here ω is the angle of inclination of the reflected shock wave with respect to the horizontal direction, i.e. $\omega_1 = \phi_3 - \theta_3 - \delta_1$ and $\omega_2 = \phi_4 - \theta_4 - \delta_2$.

Typical colour schlieren photographs showing an overall MR and an overall RR wave configuration for identical values of $M_0 = 4.96$, $\theta_1 = 28^\circ$ and $\theta_2 = 24^\circ$ are shown in figures 10(*a*) and 10(*b*), respectively. These two schlieren photographs are clear evidence that different overall wave configurations can be obtained for identical flow conditions when two asymmetric shock waves interact. The transverse waves (three-dimensional edge effects) emanating from the side edges of the reflecting plates are also seen in figures 10(*a*) and 10(*b*).

It should also be noted that based on the present analytical findings (see figure 9) the sequence of events for some values of θ_1, e.g. for $\theta_1 = 28^\circ$, encounters an overall MR wave configuration which consists of an inverse-Mach reflection wave configuration (I_nMR) for values of $\theta_2^T < \theta_2 < \theta_2^N$.

An example of such an overall MR wave configuration is shown in figure 11(*a*) for $\theta_1 = 28^\circ$, $\theta_2 = 18^\circ$ and $M_0 = 4.96$. (We emphasize again that three-dimensional edge effects contaiminte the experimental results. Consequently, they cannot be and, in fact, are not used here to verify the analytical model. They are merely presented here because of the earlier finding that they agree well with the two-dimensional theory.) For the reader's convenience a line drawing of the colour schlieren photograph shown in figure 11(*a*) is shown in figure 11(*b*) (for reasons of convenience the Mach stem length has been increased in figure 11*b*). Based on the present two-dimensional theory, the overall wave configuration for such a combination of parameters is either an overall RR or an overall MR consisting of an I_nMR and a D_iMR. In spite of the fact that the experimental evidence shown in figure 11(*a*) is not purely two-dimensional, it is clear that the overall MR wave configuration shown in it consists of a D_iMR and an I_nMR. To the best of the authors' knowledge until the present experimental study, an inverse-Mach reflection has never been reported to exist in steady flows for situations in which the flow field is free of pressure boundary conditions.

Comparisons between the experimental measurements from figure 11(*a*) and the analytical calculations based on the three-shock theory are shown in table 1. As can be seen the agreement is again surprisingly good. This fact could again imply that the three-dimensional edge effects are not too dominant in our experimental set-up. Whether this fact is general or limited to the flow Mach number at which the above comparison has been made, i.e. $M_0 = 4.96$, is yet to be investigated.

3. Conclusions

The reflection of asymmetric shock waves in steady flows has been investigated both analytically and experimentally. While the analysis was two-dimensional the experiments were not purely two-dimensional since they were contaminated with three-dimensional edge effects.

The analytical investigation was carried out using shock polars. Two extreme shock polar combinations, analogous to the well-known detachment and von Neumann conditions were identified. Their existence led to the identification of a dual-solution domain in which the overall wave configuration could be either a regular reflection (RR) or a Mach reflection (MR). As a result it was hypothesized that a hysteresis could exist in the RR $\rightarrow$ MR $\rightarrow$ RR transition process. In addition, the shock polar analysis suggested the existence of two shock wave reflection configurations, namely an inverse-Mach reflection and a strong regular reflection. These reflection wave configurations do not exist in the reflection of symmetric shock waves.

The experimental results, which as mentioned earlier were contaminated by three-dimensional edge effects, revealed a hysteresis in the RR $\rightarrow$ MR $\rightarrow$ RR transition process. The agreement between the analytical and the experimental results concerning the RR $\Leftrightarrow$ MR transition angles and the wave angles of an inverse-Mach reflection was surprisingly good in view of the fact that the analytical values were calculated using a two-dimensional theory and the experimental results were contaminated with three-dimensional edge effects. The good agreement could imply either that the three-dimensional edge effects were not too dominant in our experimental set-up, and hence that the present experiments could in practice be treated as two-dimensional or that the actual RR $\Leftrightarrow$ MR transition angles in three-dimensional steady flows are close to those of two-dimensional steady flows. Whether these two possibilities are general or limited to the flow Mach number at which the above comparisons were made, i.e. $M_0 = 4.96$, is yet to be investigated.

We would like to thank Dr Jean Claude Lengrand, Head of Laboratoire d'Aerothermique du CNRS, Meudon, France, for his encouragement and constructive remarks throughout the course of this study. We acknowledge support for this research by the Israel Science Foundation, under Grant No. 173/95.

REFERENCES

Ben-Dor, G. 1991 *Shock Wave Reflection Phenomena.* Springer.

Chpoun, A. & Lengrand, J. C. 1997 Confermation expérimentale d'un phénomène d'hystérésis lors de l'interaction de deux chocs obliques de familles différentes. *C. R. Acad. Sci. Paris* **304**, 1.

Chpoun, A., Passerel, D., Li, H. & Ben-Dor, G. 1995 Reconsideration of oblique shock wave reflection in steady flows. Part 1. Experimental investigation. *J. Fluid Mech.* **301**, 19.

Fomin, V. M., Hornung, H. G., Ivanov, M. S., Kharitonov, A. M. & Klemenov, G. P. 1996 The study of transition between regular and Mach reflection of shock waves in different wind tunnels. *Book of Abstracts of the 12th Intl Mach Reflection Symposium, South Africa.*

Han, Z. & Yin, X. 1993 *Shock Dynamics.* Kluwer.

Henderson, L. F. & Lozzi, A. 1975 Experiments on transition of Mach reflection. *J. Fluid Mech.* **68**, 139.

Henderson, L. F. & Lozzi, A. 1979 Further experiments on transition of Mach reflection. *J. Fluid Mech.* **94**, 541.

Hornung, H. G., Oertel, H. Jr. & Sandeman, R. J. 1979 Transition to Mach reflection of shock waves in steady and pseudo-steady flow with and without relaxation. *J. Fluid Mech.* **90**, 541.

Hornung, H. G. & Robinson, M. L. 1982 Transition from regular to Mach reflection of shock waves. Part 2. The steady-flow criterion. *J. Fluid Mech.* **123**, 155.

Ivanov, M. S., Gimelshein, S. F. & Beilich, A. E. 1995 Hysteresis effects in stationary reflection of shock waves. *Phys. Fluids* **7**, 685.

Ivanov, M. S., Gimelshein, S. F., Kudryavtsev, A. N. & Markelov, G. N. 1998*a* Transition for regular to Mach reflection in two- and three-dimensional flows. *Proc. 21st Intl Symp. on Shock Waves, Great Keppel Island, Australia, July 20–25 1997*, vol. 2, p. 813. Panther, Fyshwick.

Ivanov, M. S. Klemenov, G. P., Kudryavtsev, A. N., Nikiforov, S. B., Pavlov, A. A., Fomin, V. M., Kharitonov, D. V., Khotyanovsky, D. V. & Hornung, H. G. 1998*b* Experimental and numerical study of the transition between regular and Mach reflections of shock waves in steady flows. *Proc. 21st Intl Symp. on Shock Waves, Great Keppel Island, Australia, July 20–25 1997*, vol. 2, p. 819. Panther, Fyshwick.

Li, H. & Ben-Dor, G. 1996 Application of the principle of minimum entropy production to shock wave reflections. I. Steady flow. *J. Appl. Phys.* **80**, 2027.

Li, H. & Ben-Dor, G. 1997 A parametric study of Mach reflection in steady flows. *J. Fluid Mech.* **341**, 101.

Neumann, J. von 1945 Refraction, intersection and reflection of shock waves. *NAVORD Rep.* 203-45. Navy Dept., Bureau of Ordinance, Washington, DC, USA.

Neumann, J. von 1963 *Collected Works* (ed. A. H. Taub), Vol. 6. Pergamon.

Salas, M. D. & Morgan, B. D. 1983 Stability of shock waves attached to wedges and cones. *AIAA J.* **21**, 1611.

Skews, B. W. 1997 Aspect ratio effects in wind tunnel studies of shock wave reflection transition. *Shock Waves*, **7**, 373.

Skews, B. W. 1998 Oblique shadowgraph study of shock wave reflection between two wedges in supersonic flow. *Book of Abstract of the 13th Intl Mach Reflection Symposium, Beer Sheva, Israel.*

Vuillon, J., Zeitoun, D. & Ben-Dor, G. 1995 Reconsideration of oblique shock wave reflection in steady flows. Part 2. Numerical investigation. *J. Fluid Mech.* **301**, 37.